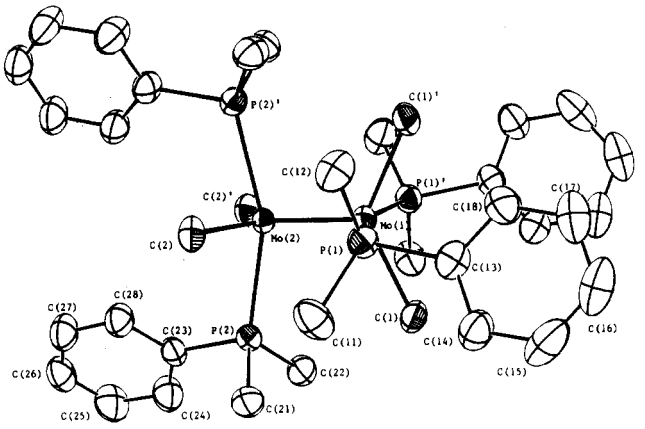

Figure 5. ORTEP drawing of the $Mo_2(CH_3)_4(PMe_2Ph)_4$ (**3**) molecule. Atoms are represented by their ellipsoids at the 50% probability level.

electron rich. The Mo–P bond distance presumably decreases because more Mo → P π bonding occurs. Both π and δ orbitals of the Mo–Mo bond could do this, thus lengthening the Mo–Mo bond.

Concluding Remarks

Synthesis of **1** revealed the ability of a Grignard reagent to act as either an alkylating or a halogenating agent. Synthesis of pure $Mo_2(CH_3)_4(PR_3)_4$ complexes, which are free of all halogen-containing contaminants, requires the use of $(CH_3)_2Mg$ prepared from $(CH_3)_2Hg$ in these systems. The structural investigations of **2** and **3** coupled with ^1H NMR evidence suggest that the material originally used to obtain the structure of **2** was actually a mixture of $Mo_2Cl_4(PMe_3)_4$ and $Mo_2(CH_3)_4(PMe_3)_4$. The Mo–C distances in Mo_2^{4+} core dimers are consistently 2.25 ± 0.02 Å. The Mo radius for $Mo_2(CH_3)_4(PR_3)_4$ is 0.05 Å larger than that of $Mo_2Cl_4(PR_3)_4$ species and indicates a more electron-rich Mo_2^{4+} core for alkyl-containing compounds.

Acknowledgment. We thank the National Science Foundation for financial support.

Supplementary Material Available: Tables for compounds **1–3** of all bond distances and angles, thermal parameters, and hydrogen coordinates and an ORTEP drawing of the second molecule of **3** (20 pages); tables of observed and calculated structure factors for **1–3** (57 pages). Ordering information is given on any current masthead page.

Contribution from the Chemistry Department, The Ohio State University, Columbus, Ohio 43210, and Department of Chemistry, University of Warwick, Coventry CV4 7AL, England

Transition-Metal Complexes of Superstructured Cyclidene Macrobicycles: Structural Features and Their Chemical Consequences. 3.[1] Cyclidenes with Long Polymethylene Bridges

Nathaniel W. Alcock,*,† Peter A. Padolik, Graham A. Pike, Masaaki Kojima, Colin J. Cairns, and Daryle H. Busch*,‡

Received November 28, 1989

The syntheses and X-ray structure determinations are reported for lacunar cyclidene complexes bridged by $-(CH_2)_9-$ (**9**) and $-(CH_2)_{10}-$ (**10**) chains. Correlation of these results with those for $-(CH_2)_8-$ and $-(CH_2)_{12}-$ bridges show how the transformations from the flat cavity increasing in width from $-(CH_2)_3-$ through $-(CH_2)_8-$ to the tall narrow cavity for $-(CH_2)_{12}-$ takes place through graduated conformational changes at the nitrogen atoms to which the bridging groups are attached. These changes can also be observed in ^{13}C NMR spectra, demonstrating that conformations are present in solution similar to those found in the solid state. Correlation of ^{13}C chemical shift with chain length over the range $-(CH_2)_n-$ (n = 3–10, 12) shows that some resonances are strongly influenced by cavity width. Other resonances show a small-scale alternation between n-odd and n-even, associated with the distortions required in bridges formed from even-membered chains. Crystal data: $C_{29}H_{50}N_6P_2F_{12}Ni.C_3H_6O$ (**9**), triclinic, $P\bar{1}$, a = 11.298 (6) Å, b = 13.615 (9) Å, c = 14.608 (10) Å, α = 75.48 (5)°, β = 73.32 (5)°, γ = 73.56 (5)°, Z = 2; $C_{30}H_{52}N_6P_2F_{12}Ni.C_2H_3N$ (**10**), orthorhombic, $P2_12_12_1$, a = 10.221 (4) Å, b = 13.723 (11) Å, c = 29.255 (16) Å, Z = 4.

Introduction

Previous studies in these laboratories[2] have established that the O_2 affinities of the lacunar cyclidenes (Figure 1) are strongly dependent on the shape and size of the molecular voids within which the dioxygen binds and that these are controlled by the nature of the substituents R^1–R^3. In a systematic study of this control, we examined the structures of the cyclidenes with polymethylene bridges $-(CH_2)_n-$, with n = 3–8 and 12.[1] The main trend in this series involves a linear increase in the cavity width as n goes from 3 to 8, culminating in one of the widest and flattest cavities yet identified (Figure 2a).

In remarkable contrast, in the cyclidene with a $-(CH_2)_{12}-$ bridge, the void is both narrow and extremely tall (Figure 2b). This difference does not merely result from the flexibility of the longer chain giving it the opportunity to stretch further and double back on itself. A substantial alteration has also taken place in the primary cyclidene unit. Rotation about the C–N bond of the nitrogen to which the bridge is attached is restricted by its partial double-bond character. In the absence of steric constraints, the substituents at this nitrogen (here the CH_3 and $-(CH_2)_n-$ chain) are oriented so that one group points directly away from the metal ion.[3,4] The bridge can take up either orientation, leading to the isomers described as "lid-on" and "lid-off" (Figure 3a,b).[3] The change from a $-(CH_2)_8-$ chain to a $-(CH_2)_{12}-$ chain involves the conversion from the lid-off to the lid-on form (compare the positions of C17 and C26 in Figure 2a with those of C11 and C11a in Figure 2b). This is potentially of particular significance in

*To whom correspondence should be addressed.
† University of Warwick.
‡ Department of Chemistry, The University of Kansas, Lawrence, KS 66045-0046.

(1) Part 2: Alcock, N. W.; Lin, W.-K.; Cairns, C.; Pike, G. A.; Busch, D. H. *J. Am. Chem. Soc.* **1989**, *111*, 6630.
(2) For a summary, see: Busch, D. H. In *Oxygen Complexes and Oxygen Activation by Transition Metals*; Martell, A. E., Sawyer, D. T., Eds.; Plenum Publishing Corp.: New York, 1988.
(3) Herron, N.; Nosco, D. L.; Busch, D. H. *Inorg. Chem.* **1983**, *22*, 2970.
(4) Alcock, N. W.; Cairns, C.; Jircitano, A. J.; Nosco, D. L.; Busch, D. H. *Acta Crystallogr., Sect. C* **1987**, *C43*, 2069.

0020-1669/90/1329-2599$02.50/0

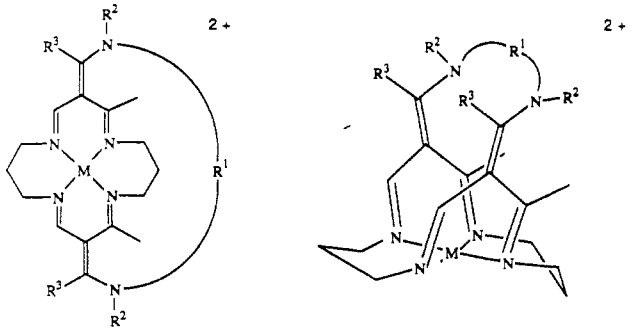

Figure 1. Structural diagram of a bridged cyclidene: (a) flat projection; (b) 3-dimensional representation.

relation to ligand binding because, in the lid-on form, the methyl substituents greatly reduce the accessible width of the cavity; these complexes typically have a C···C distance of no more than 4 Å.

In this paper we examine in detail the transition from the lid-off $-(CH_2)_8-$ to the lid-on $-(CH_2)_{12}-$ complex, with the aid of new structural results for the complexes with nine and ten methylene groups in the bridge. The paper also explores the systematic correlation of ^{13}C NMR spectra and structure, to throw light on cyclidene conformations in solution and to establish the potential of the spectra for studying complexes whose solid-state structures are unknown. These correlations have been the subject of previous work,[5] but with the benefit of precise knowledge of the structures of polymethylene-bridged cyclidenes,[1] we can refine the analysis both of small-scale shifts and of the major changes that take place as the chain length increases.

Results and Discussion

Preparations and Crystal Structures. Previous attempts to synthesize cyclidenes with long polymethylene bridges have encountered difficulties due to incomplete reaction.[6] This problem has been overcome by modification of the experimental procedure and by more careful purification (at the cost of somewhat reduced yields in the final bridging reaction), and we have successfully synthesized and determined the crystal structures of **9** and **10** (I, M = Ni^{2+}, counterion = PF_6^-, $R^2 = R^3 =$ Me, $R^1 = -(CH_2)_9-$ and $-(CH_2)_{10}-$, respectively).[7]

Figure 4 shows views of **9** and **10**, and Table I lists the key structural parameters defining the cyclidene units (identified in Figure 5, with the notation used in this section); information for **8a** and **12** (from ref 1) is included for comparison. A remarkable fact is immediately apparent. The transition from wide/lid-off to narrow/lid-on is *graduated*, not sharp, even though each individual N3 is itself lid-on or lid-off. Both **9** and **10** show disorder at one N3 (labeled N6 in Figure 4a,d). For **9**, the other N3 is lid-off, and so **9** can be described as one-fourth converted from lid-off to lid-on. Complex **10** has the second N3 lid-on and is therefore three-fourths converted. The shape parameters for the cyclidene unit (Table I) show the progress of the conversion, with angles α and β and C···C and N···N distances across the cavity all decreasing in the order **8**, **9**, **10**, **12**. In **10**, the bond lengths for the cyclidene unit show some anomalies, though the values lie within the fairly large range previously identified.[1,8] However, the esd's of these distances (even after averaging) are too large for much weight to be put on the anomalies.

Table I. Principal Dimensions and Structural Prameters[a] for **8**,[b] **9**, **10**, and **12**[b]

	complex			
	8	**9**	**10**	**12**
metal ion	Cu^{2+}	Ni^{2+}	Ni^{2+}	Ni^{2+}
M–N	1.97	1.89	1.89	1.88
$M/N_1–N_4$	0.04	0.05	0.09	0.10
$N–C_1/C_2$	1.30	1.26	1.28	1.30
$C_1/C_2–C_3$	1.43	1.46	1.43	1.43
$C_3–C_4$	1.44	1.44	1.41	1.43
$C_4–N_3$	1.31	1.32	1.38	1.31
α	110.2	101.4	100.2	90.5
β	69.4	57.9	56.2	47.2
γ	24.9	26.6	22.0	21.2
$C_4\cdots C_4'$	7.75	7.29	7.08	6.14
$N_3\cdots N_3'$	7.82	7.31	6.81	5.80
$M\cdots C_{mid}$[c]	4.41	7.28	6.88	9.92
$M\cdots Me(N_3)$[d]	6.80	6.62	4.84	4.65
		4.83	4.89	
		6.63	6.59	

[a] Average values, deg and Å; esd's < 0.02 Å, 1.5°. See Figure 5 for identification of atoms and parameters. [b] Taken from ref 1 (compound **8a**). [c] Central carbon for *n*-odd, midpoint of cental C–C bond for *n*-even. [d] Carbon atom of the CH_3 group attached to N_3.

The chain conformations for **9** and **10** are identified by the torsion angles listed in Table II.[9] The angle ϵ (the CCN3C angle) differentiates very clearly between the lid-on and the lid-off conformations, with the individual values all lying close to the ideals of 180 and 0°, respectively. The expected mixture of gauche and anti conformations is found along the chain for **10** and the well-defined portions of **9**, apart from the 120° angles typical for the CNCC bond.[1] The overall orientations of the chains in relation to the metal ions are rather different, as can be seen from Figure 4b,c,e,f. For **9**, the chain stands up almost vertically above the metal (as in **12**), while for **10** it is much more oblique but in the direction opposite from that typical for the lid-off complexes. Molecular mechanics calculations on cyclidenes with polymethylene bridges[10] indicate that such long chains have many alternative orientations of almost equal energy. Therefore, this difference is probably not of great significance.

Correlation of ^{13}C NMR Spectra and Structure. The ability of ^{13}C NMR to detect structural changes is clearly demonstrated by comparison of selected resonances over the entire range of polymethylene-bridged complexes Figures 6–12 and Table III). These chemical shifts show a bewildering response to variation in chain length. However, a detailed analysis allows three structural trends to be identified from these spectra, relating to (i) the lid-off/lid-on transformation from **8** to **12**, (ii) the overall effects of the changing shape of the cyclidene cavity between **3** and **12**, and (iii) a remarkable alternation in the chemical shifts for certain peaks between complexes with bridges containing odd and even numbers of carbon atoms.

Following previous examination of the ^{13}C NMR spectra for **3**–**8**[11,12] and study of the ^{13}C–^1H 2-D correlation spectra, the ^{13}C peaks for all of the complexes can be assigned to individual carbon atoms as identified in Figure 6 (with some ambiguity for the central carbon atoms of the $-(CH_2)_n-$ chain, whose resonances fall close together).

Several ^{13}C resonances of **9** and **10** display peak broadening at room temperature, most notably for a, k, and l (Figures 7 and 8). At 340 K, the resonances coalesce into sharp lines in most cases, and the overall appearances of the spectra are similar to those of the shorter polymethylene chain complexes. However,

(5) Meade, T. J.; Fendrick, C. M.; Padolik, P. A.; Cottrell, C. E.; Busch, D. H. *Inorg. Chem.* **1987**, *26*, 4252.
(6) Cairns, C.; Busch, D. H. Unpublished results.
(7) For clarity, we continue the scheme used in ref 1 for identifying each complex by its chain length. In this paper, all the compounds **3**–**10** and **12** have M = Ni^{2+} and $R^2 = R^3 =$ Me. Some of the complexes whose crystal structures were reported in ref 1 have different metals and substituents.
(8) Alcock, N. W.; Lin, W. K.; Jircitano, A.; Mokren, J. D.; Corfield, P. W. R.; Johnson, G.; Novotnak, G.; Cairns, C. J.; Busch, D. H. *Inorg. Chem.* **1987**, *26*, 40. Note that compound **4** in this paper should correctly be named (6,13-diacetyl-5,12-dimethyl-1,4,8,11-tetraazacyclotetradeca-4,6,11,13-tetraenato(2−)-κ^4N)nickel(II), rather than as the 5,14-dimethyl complex.
(9) The values for the disordered part of the chain in **9** are unreliable because several alternative chain routes can be traced through the observed atomic positions. A similar problem was encountered in **12**.[1]
(10) Part 4 of this series, to be published.
(11) Busch, D. H.; Olszanski, D. J.; Stevens, J. C.; Schammel, W. P.; Kojima, M.; Herron, N.; Zimmer, L. L.; Holter, K. A.; Mocak, J. *J. Am. Chem. Soc.* **1981**, *103*, 1472.
(12) Herron, N.; Chavan, M. Y.; Busch, D. H. *J. Chem. Soc., Dalton Trans.* **1984**, 1491.

Table II. Chain Torsion Angles (deg) for **9** and **10**

	bond							
			along chain, outward from N_3 →					
complex	CCCN (δ)	CCNC (ϵ)	CNCC	NCCC	CCCC	CCCC	CCCC	CCCC
9	−45.7	−10.1	−125.3	50.7	168.3	−97.6	3.0	
	39.7	−169.4[a]	−119.2	58.7	−85.8	−113.7	−178.0	
		12.1						
10	−44.4[b]	179.1	106.3	−50.3	177.8	−160.0	61.5	58.1
	45.3	7.1[b]	115.4	−65.2	179.3	165.8	−150.5	
		178.9	−115.8	58.8	−171.6	175.8	170.1	

[a] For **9**, the disordered chain takes at least three alternative routes. Apart from the well-defined lid-on/lid-off disorder at N6, the sequence of torsion angles corresponds to the lid-on route shown in the solid bonds in Figure 4. [b] For **10**, two alternative routes are well defined and both sequences of torsion angles are listed.

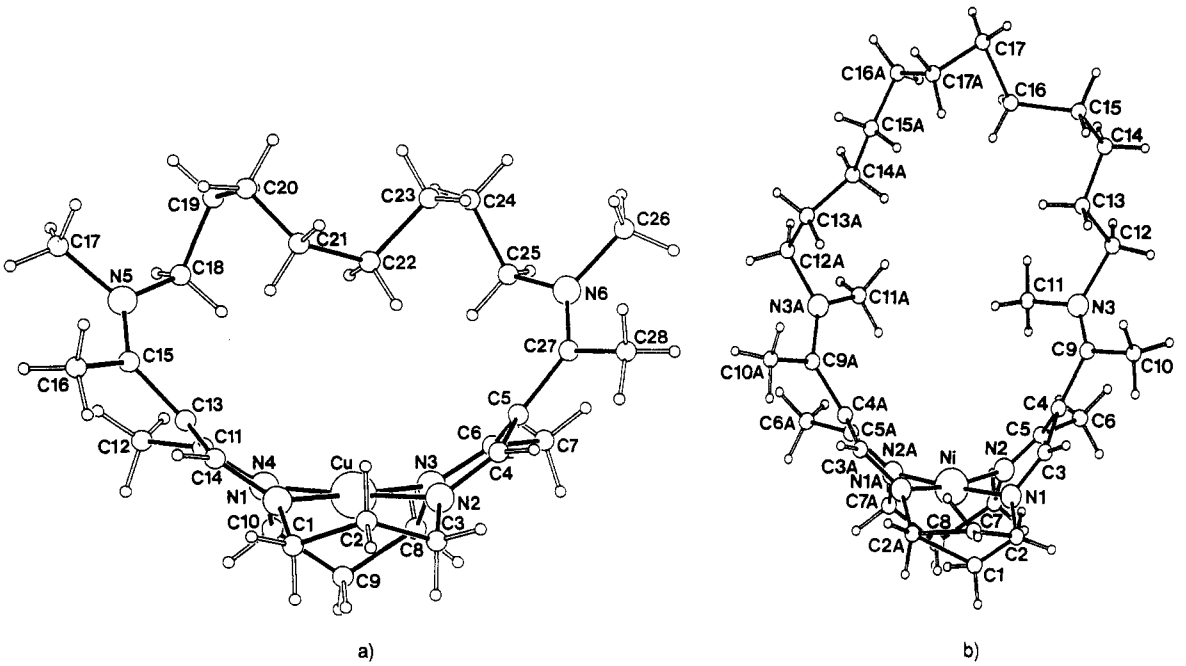

Figure 2. (a) Cyclidene unit bridged by $-(CH_2)_8-$ chain (**8**) (**8a** from ref 1). (b) Cyclidene unit bridged by $-(CH_2)_{12}-$ chain (**12**) (**12** from ref 1).

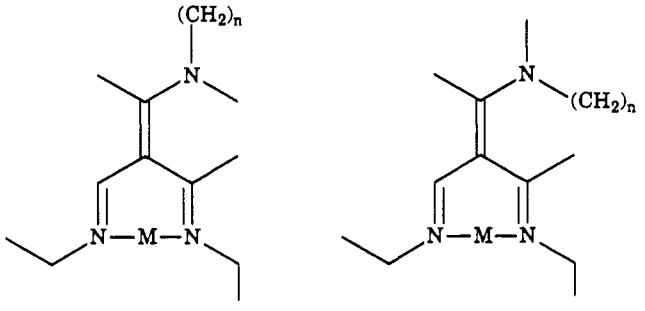

a) lid-on **b) lid-off**

Figure 3. Isomers of bridged cyclidenes: (a) lid-on; (b) lid-off.

at 240 K, the spectra are seen to be extremely complex, with at least three resonances for each peak. While the ^1H NMR spectra of **9** and **10** show a similar effect, the complexity of the spectra and the limited changes in chemical shifts for the isomeric species make this technique less informative. The complicated nature of the low-temperature spectra is most clearly demonstrated for complex **9**. An expanded view of 15–60 ppm region of the ^{13}C spectrum for this complex at 240 K is shown in Figure 7d. Although the chemical shift of each carbon is unique for each isomeric species at low temperature, the resonances that are broadened at room temperature are made up of lines whose chemical shifts are most divergent at 240 K, and the resonance for carbon k provides a striking example. The expanded low-temperature spectrum of **9** (Figure 7d) shows three peaks in the 38–46 ppm range attributable to the resonance for carbon k in its various isomeric forms. A simple averaging of the chemical shifts for these peaks support this; the average value of 41.0 ppm is comparable to the chemical shift of 41.4 ppm for the coalesced peak measured at 340 K. Thus, it is evident that the chemical shift for this carbon differs by ~8 ppm between the two conformations.

The fluxional behavior observed at room temperature arises from the interconversion of *lid-on* and *lid-off* conformers. Since their interconversion takes place by rotation about the C–N bond, the carbons bonded to the bridging nitrogen experience the most significant change in chemical environment and chemical shift upon isomerization. Thus, the resonances for carbons a, k, and l show the greatest effects. It should be noted that interconversion between the *lid-off* and *lid-on* forms results in conformational changes throughout the *entire* macrocycle, affecting every resonance in the NMR spectra of the complexes. However, for most of these resonances, this is not profound enough to produce significant line broadening.

The low-temperature splitting patterns of resonance k for **9** and **10** both display a close doublet of peaks and a singlet. However, the patterns are mirror images of each other. The spectrum for **9** shows a doublet at high field indicating two different lid-off conformations, and a singlet at low field, corresponding to one lid-on conformation. This is explained by the presence of a mixture of the lid-off/lid-off isomer (producing one "lid-off" resonance) and the lid-on/lid-off isomer (producing a second lid-off resonance and one lid-on resonance). In **10**, the low-field singlet and high-field doublet can be similarly interpreted as resulting from a mixture of the lid-on/lid-on and lid-on/lid-off isomers. This

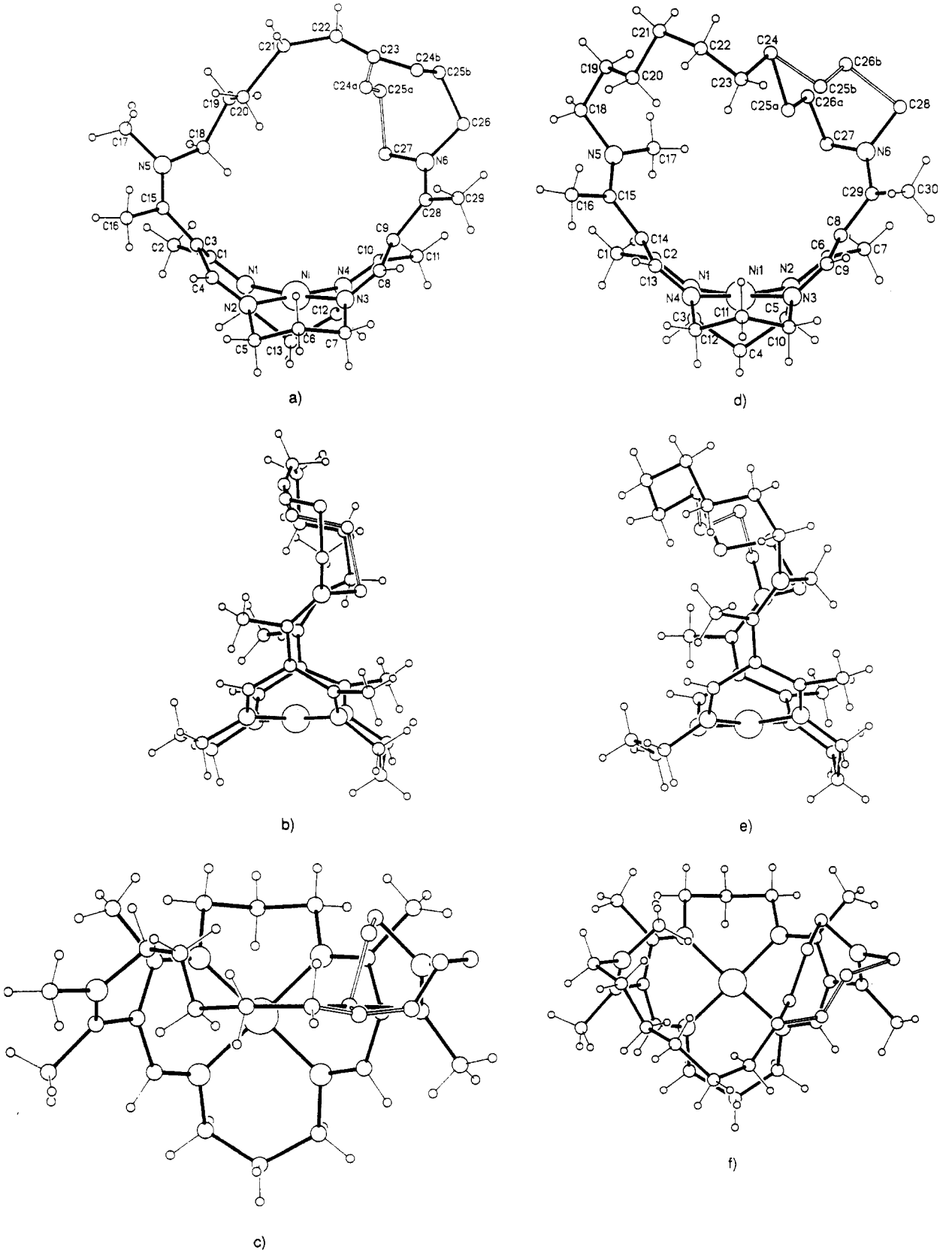

Figure 4. Views and atomic numbering of (a–c) the cation of **9** and of (d–f) that of **10**. In c and f, the cation is viewed perpendicular to the MN_4 plane, to show the relative orientation of chain and metal ion.

corresponds precisely to the crystal structure results, providing excellent evidence that the basic isomer pattern observed in the crystal structure for each complex persists in solution.

The large upfield shift of the resonance for the methyl carbon k of **9**, accompanying isomerization from the lid-off to the lid-on form, can be understood on the basis of this carbon atom's environment. From Figure 4a, the methyl group containing k points *away* from the pocket in the *lid-off* case (C17 and C26), but in the *lid-on* conformation (Figure 4b), it is directed *into* the pocket (C27). Therefore, the upfield shift for the k resonance in the *lid-on* isomer is due to a deshielding interaction with the Ni^{2+} metal center.[5] The Me···Me distances (Table I) are consistent with this scenario, with values of 6.6–6.8 Å for the lid-off isomer and 4.6–4.8 Å for the lid-on.

Table III. ^{13}C NMR Chemical Shift Data and Assignments[a] for Complexes **3–10** and **12**

	δ								
carbon[a]	**3**[c]	**4**[d]	**5**[d]	**6**[d]	**7**[d]	**8**[d]	**9**[e]	**10**[e]	**12**[e]
a	171.9	171.8	173.7	173.3	175.7	174.4	175.7[f]	174.7[f]	174.1[f]
b	168.5	169.0	167.2	167.5	166.9	167.3	167.7	168.1	168.2
c	159.4	160.6	159.1	160.1	159.7	160.4	160.0	160.0	160.0
d	113.9	112.7	112.0	110.9	110.8	110.5	111.7	111.9	112.2
e	55.1	55.2	56.1	56.1	56.1	56.6	56.7	56.5	56.3
f	50.5	50.2	51.2	51.3	51.8	51.8	51.9	51.7	51.5
g	29.9	30.1	30.4	30.3	29.9	29.9	30.3	30.6	30.9
h	31.5	31.4	30.7	30.7	30.9	30.9	31.1	31.0	30.8
i	19.9	20.5	20.3	20.7	20.5	21.0	21.0	21.3	21.4
j	19.7	19.5	20.0	19.7	20.4	20.0	20.7	20.6	19.9
k	42.4	41.2	41.2	40.2	39.0	39.6	41.4[f]	41.9[f]	42.8[f]
l	55.9	57.2	57.9	57.5	57.1	57.1	57.7[f]	56.1[f]	56.2[f]
m	25.2	24.1	(27.1)	25.0	(27.1)	(25.8)	27.3	27.7	27.6[f]
n			(23.5)	24.0	(26.4)	(24.9)	(28.5)	(28.3)	(29.2)
o					(25.4)	(22.1)	(27.9)[f]	(27.8)[f]	(28.4)[f]
p							(26.2)[f]	(26.0)[f]	(27.9)[f]
q									(26.9)[f]

[a] Chemical shift values in parentheses denote uncertain assignments. [b] For carbon atom identification scheme, see Figure 6. [c] Spectrum obtained at 300 K, correcting the values given in ref 12. [d] Chemical shift values taken from ref 11. [e] Spectra obtained at 340 K. [f] Resonances broadened at room temperature.

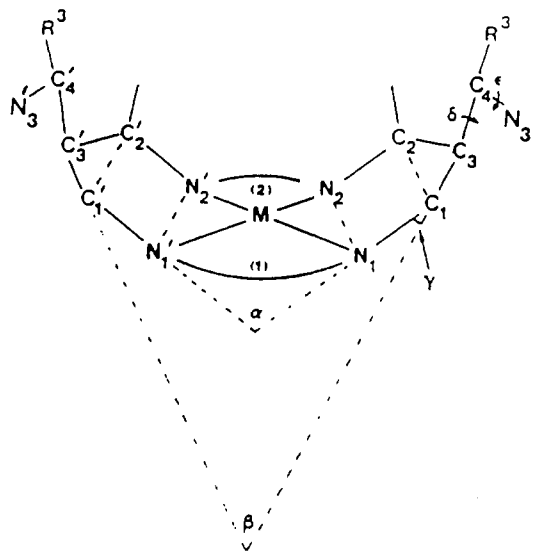

Figure 5. Structural parameters defining the cyclidene unit.

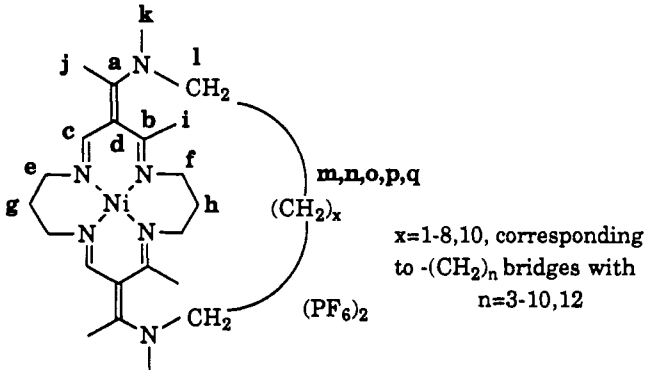

Figure 6. Identification of carbon atoms for ^{13}C spectra.

Apart from the splitting of resonance k, the low-temperature spectrum of **10** is much more complex than that of **9**, though its limiting high-temperature spectrum is very similar (Figure 8). This particularly affects the resonances arising from the $-(CH_2)_n-$ carbon atoms. We attribute this to the ability of the bridge to take up a number of alternative conformations of similar stability. Similarly, the spectrum for **12** shows many splittings at low temperature (Figure 9). Interestingly, this spectrum also shows splitting for resonance k, indicating that in solution it can adopt a lid-on/lid-off conformation, as well as the lid-on/lid-on one.

The effects on the NMR spectra of the changing shape of the lacunar cyclidene cavity (trend ii) are well illustrated by plots of chemical shift vs the number of methylene units n for carbons d, e, f, and k (Figure 10). When n increases from 3 to 8, d and k exhibit downfield shifts while e and f move upfield. However, dramatic reversals occur in these trends from $n = 9$ to 12. The principal determinant of these shifts appears to be the changing width of the cavity. Figure 11 illustrates this most clearly in the nearly linear correlation of chemical shift and width (N3···N3′)[1] for d. Similar correlations are found for e, f, and k, but these are more strongly affected by the odd–even alternation described below. The direct effect on atom d of changing the cavity width is to move that atom with respect to the metal atom, thereby altering the local field it experiences. The previous suggestion[13] that the C4–N torsion angle (ϵ) controls the chemical shift for d is not supported by the crystal structure results,[1] which show that ϵ has a very limited range of variation (10–21°).

It is reasonable that e and f are particularly influenced by the cavity width because their positions with respect to the metal atom are directly affected by the changes in the parameter α. Since they are adjacent to the donor nitrogen atoms, rotation about the metal–nitrogen bond (necessary to change α) will produce a precisely correlated movement of these atoms.

The other carbon atoms are, of course, also influenced by changes in the cyclidene unit. However, they are more strongly affected by an n-odd/n-even alternation, which is particularly clear for a, i, and j (Figure 12). It should be noted that this effect is small, some 0.2 ppm peak to trough, whereas the change in width produces shifts as great as 5 ppm. This alternation has previously been noted,[14] and an explanation was suggested in terms of the zigzag nature of an extended $-(CH_2)_n-$ chain. With the knowledge that the chains have much more complex conformations, this is no longer tenable. However, a geometrical origin must certainly be sought for this remarkable effect. It is known that a $-(CH_2)_n-$ chain with n-odd forms a much more symmetrical bridge and has fewer low-energy conformations than does a chain with n-even.[1] This arises because an ideal sequence of torsion angles leads, in the n-odd case, to the final carbon atom being oriented correctly for bonding, but with n-even the final atom is positioned incorrectly. The consequence is that for n-even chains any ideal conformation must be distorted to allow the bridge to form. Examination of the torsion angles (Table IV in ref 8) shows that the angle δ (for the bond between a and d) is particularly affected

(13) Goldsby, K. A.; Meade, T. J.; Kojima, M.; Busch, D. H. *Inorg. Chem.* **1985**, *24*, 2588.
(14) Marvel, C. S.; Sekera, B. C. *Org. Synth.* **1940**, *20*, 50.

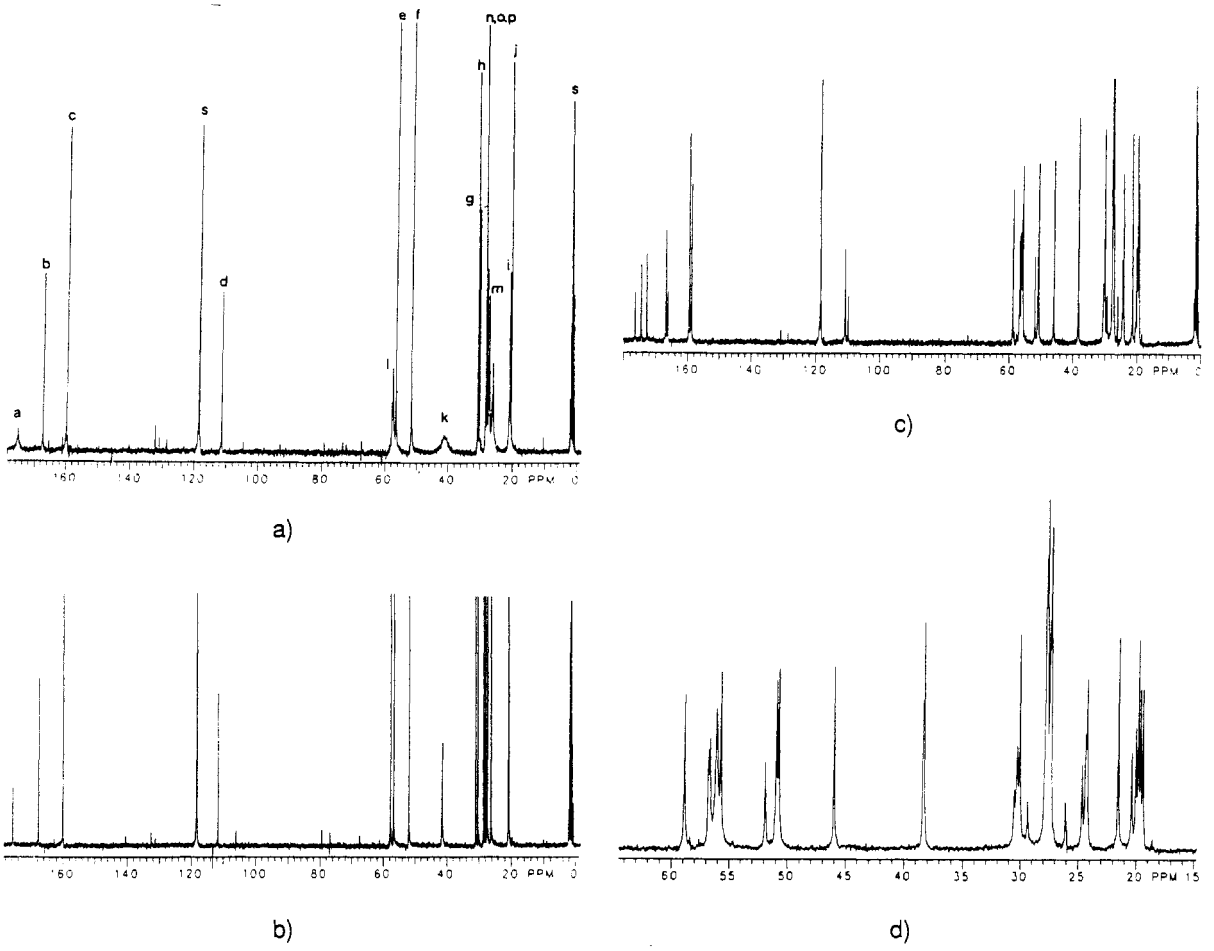

Figure 7. ^{13}C NMR spectra for **9**: (a) at room temperature, with assignments (s indicates solvent peaks); (b) at 340 K; (c) at 240 K; (d) at 240 K, expanded section of (c).

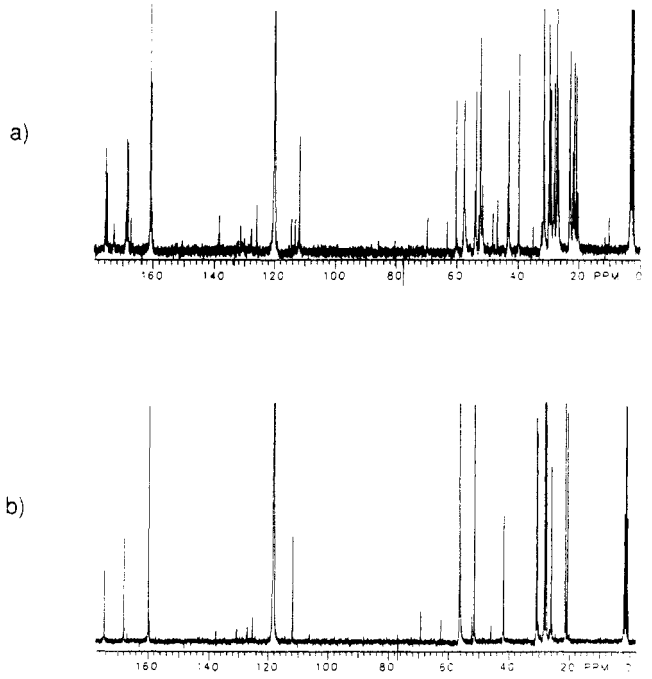

Figure 8. ^{13}C NMR spectra of **10**: (a) at 240 K; (b) at 340 K.

(Figure 13). The values of δ lie between 30 and 45°, and between $n = 3$ and 8, these values are alternately large and smaller as n increases. The observed values of δ are undoubtedly affected by crystal packing and other structural effects, as is shown by the variations in δ between different structures with the same chain length. For the compounds in solution, the values of δ will be averaged over the accessible conformations, and these mean values can be expected to show more regularity.

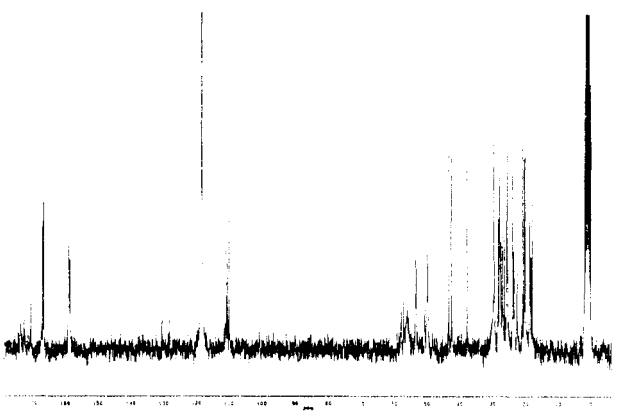

Figure 9. ^{13}C NMR spectrum for **12** at 240 K.

The atoms with most marked alternation in their chemical shifts are all in or close to the a–d bond. It is not surprising that the chemical shifts for i and j are most affected by alternation and least affected by the changes in cavity width. As terminal methyl groups, they are relatively insensitive to electronic effects in the conjugated c–d–b–a system.

Experimental Section

Syntheses. 1,9-Bis(*p*-tolylsulfonyl)nonane and 1,10-Bis(*p*-tolylsulfonyl)decane. These compounds were synthesized by using *p*-toluenesulfonic acid and the appropriate diol following a published method.[14]

[(2,3,13,14,16,22-Hexamethyl-3,13,17,21,24,28-hexaazabicyclo[13.7.7]nonacosa-1,14,16,21,23,28-hexaene-κ^4N)nickel(II)] Hexafluorophosphate (9). A 1.4-g sample of 1,9-bis(*p*-tolylsulfonyl)nonane (3.0

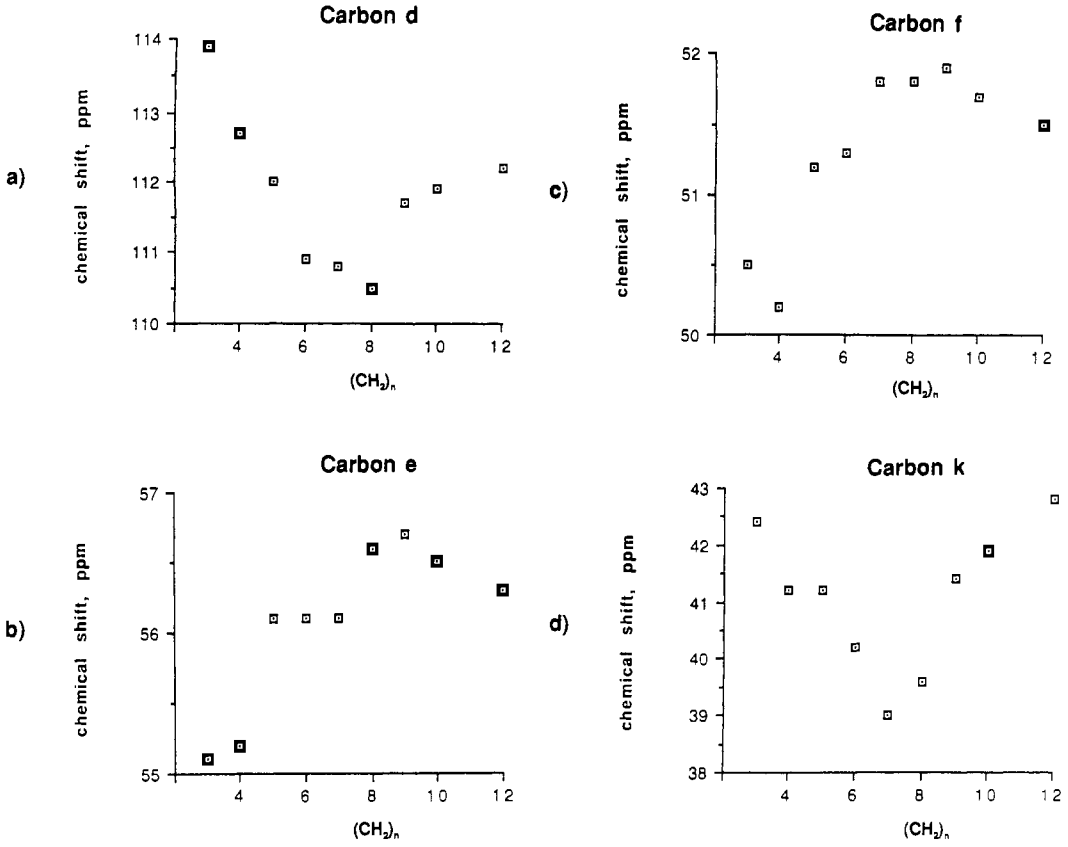

Figure 10. Variation of ^{13}C chemical shift with n for carbon atoms d, e, f, and k.

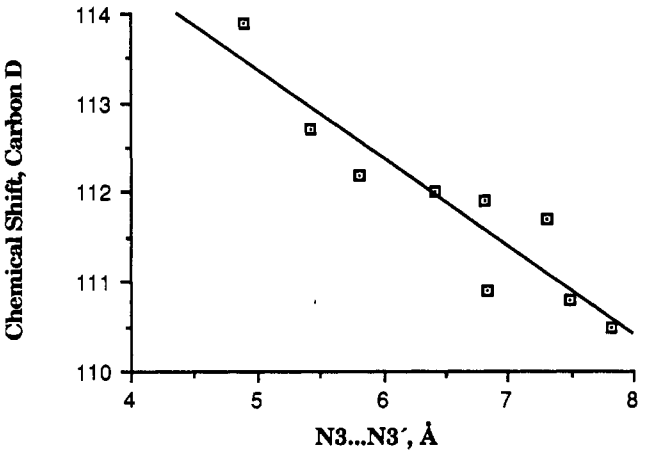

Figure 11. Correlation of ^{13}C NMR chemical shift and N3···N3′ cavity width for d.

mmol) was dissolved in 250 mL of acetonitrile. In a separate flask, 2.1 g of [Ni(MeNEthi)$_2$[16]cyclidene](PF$_6$)$_2$[15] was dissolved in 240 mL of acetonitrile. To this solution was added 0.14 g of sodium metal (2.1 equiv) in 10 mL of methanol. Both solutions were dripped simultaneously into a reservoir containing 400 mL of boiling acetonitrile over a 4-h period. The reaction was allowed to reflux for 24 h, at which point a white precipitate presumed to be sodium tosylate was observed. After being cooled to room temperature, the reaction mixture was filtered, the solvent volume was reduced, and the concentrated solution was passed through a neutral alumina column that used acetonitrile as the eluent. The column chromatography step was repeated to remove any residual tosylate salts, the solvent volume was reduced, and ethanol was added until the solution was persistently cloudy. A few drops of acetonitrile were added to regain a clear solution, which was then chilled in a freezer for 12 h. The resultant orange microcrystalline product was filtered out, washed with ethanol, and dried in vacuo. Yield: 0.9 g (36%). Anal.

(15) Schammel, W. P.; Zimmer, L. L.; Busch, D. H. *Inorg. Chem.* **1980**, *19*, 3159.

Table IV. Selected ^{13}C NMR Chemical Shift Values for Isomeric Species of **9**, **10**, and **12** at 240 K

	δ		
carbon[a]	**9**	**10**	**12**
a	176.4	175.8	173.4
	174.7	175.0	172.4
	173.1	173.0	170.4
k	46.0	43.6	43.2
	38.3	42.9	42.4
	38.2	40.0	37.6
l	58.9	60.2	55.8[b]
	56.8	54.2	53.2
	56.6	54.0	

[a] For carbon atom identification scheme, see Figure 6. [b] Broad signal.

Table V. Data Collection and Refinement Details for X-ray Structural Determination of the Nickel(II) Complexes **9** and **10**

	9	**10**
empirical formula	$NiC_{29}H_{50}N_6P_2F_{12}\cdot C_3H_6O$	$NiC_{30}H_{52}N_6P_2F_{12}\cdot CH_3CN$
fw	831.4 + 58.1	845.4 + 41.0
cryst system	triclinic	orthorhombic
space group	$P\bar{1}$	$P2_12_12_1$
a, Å	11.298 (6)	10.221 (4)
b, Å	13.615 (9)	13.723 (11)
c, Å	14.608 (10)	29.255 (16)
α, deg	75.48 (5)	90
β, deg	73.32 (5)	90
γ, deg	73.56 (5)	90
V, Å^3	2033 (2)	4103 (3)
Z	2	4
dens(calcd), g/cm^3	1.45	1.40
λ, Å	0.71073	0.71069
μ(Mo Kα), cm^{-1}	6.3	6.4
no. of individual rflcns	6388	4051
no. of rflcns with $I/\sigma(I) \geq 2.0$	3526	2526
cryst dimens, mm	0.22 × 0.33 × 0.34	0.55 × 0.48 × 0.14
R, R_w	0.090, 0.096	0.080, 0.082
T, K	290	293

Table VI. Atomic Coordinates ($\times 10^4$)

	x	y	z		x	y	z
			9				
Ni	2922.3 (11)	2072.0 (9)	6676.2 (9)	C8	2270 (11)	2804 (8)	8385 (8)
P1	−1996 (3)	2817 (2)	5817 (2)	C9	1002 (9)	3310 (7)	8231 (7)
P2	3228 (4)	2765 (3)	1643 (3)	C10	985 (10)	3788 (7)	7219 (8)
F11	−2702 (8)	2365 (7)	6840 (5)	C11	104 (12)	4843 (8)	7044 (8)
F12	−1306 (12)	3286 (6)	4791 (6)	C12	1850 (12)	4005 (7)	5539 (7)
F13	−738 (6)	2479 (6)	6182 (7)	C13	2789 (11)	3422 (8)	4799 (8)
F14	−3253 (10)	3089 (8)	5479 (7)	C14	2431 (11)	2448 (8)	4766 (7)
F15	−1665 (8)	1746 (5)	5486 (5)	C15	2331 (10)	−1025 (7)	6651 (7)
F16	−2318 (9)	3902 (5)	6133 (5)	C16	3302 (13)	−2038 (9)	6742 (13)
F21	4306 (10)	2274 (9)	2160 (9)	C17	754 (13)	−2042 (8)	6918 (8)
F22	2008 (11)	3227 (15)	1307 (10)	C18	85 (11)	−148 (9)	6911 (8)
F23	2861 (12)	3649 (8)	2223 (10)	C19	−1035 (19)	−166 (14)	7823 (17)
F24	3662 (18)	1911 (12)	1099 (10)	C20	−623 (16)	−474 (15)	8609 (17)
F25	2461 (12)	2097 (11)	2508 (8)	C21	−1977 (29)	−209 (25)	9605 (14)
F26	4016 (14)	3355 (9)	813 (8)	C22	−2583 (32)	609 (26)	10215 (25)
N1	2529 (7)	1676 (6)	5673 (5)	C23	−2407 (60)	1373 (52)	10399 (44)
N2	4065 (7)	766 (6)	6802 (6)	C24A	−1824 (30)	1582 (24)	9844 (23)
N3	3182 (8)	2392 (6)	7774 (6)	C24B	−2538 (35)	2276 (35)	10559 (27)
N4	1768 (8)	3390 (5)	6531 (6)	C25A	−2584 (35)	2560 (30)	9078 (27)
N5	1156 (10)	−1076 (6)	6799 (6)	C25B	−3132 (34)	3126 (30)	10188 (27)
N6	−1236 (9)	3623 (7)	8966 (7)	C26	−2347 (13)	4018 (12)	9728 (10)
C1	2299 (9)	800 (8)	5724 (7)	C27	−1549 (11)	3336 (11)	8155 (10)
C2	1823 (11)	595 (8)	4948 (8)	C28	−43 (12)	3518 (8)	9025 (8)
C3	2730 (9)	−80 (7)	6433 (7)	C29	198 (13)	3537 (12)	9980 (9)
C4	3788 (9)	−55 (8)	6786 (8)	O001	7319 (10)	4666 (8)	1968 (7)
C5	5263 (10)	638 (9)	7075 (10)	C002	5222 (12)	4939 (9)	2400 (9)
C6	5036 (10)	961 (10)	8029 (10)	C001	5882 (13)	4965 (11)	3452 (11)
C7	4428 (9)	2101 (9)	8043 (9)	C003	5202 (14)	5265 (11)	1865 (11)
			10				
Ni1	5000	6124.6 (11)	1986.8 (5)	C8	3891 (15)	4130 (10)	1645 (5)
P1	6634 (8)	3870 (5)	91 (2)	C9	5094 (17)	4446 (9)	1472 (5)
P2	188 (4)	1039 (3)	2249 (1)	C10	7101 (14)	5282 (11)	1435 (5)
F11	6989 (18)	3576 (10)	599 (4)	C11	7245 (14)	6212 (12)	1156 (6)
F12	6235 (19)	4142 (11)	−419 (4)	C12	7011 (14)	7126 (11)	1463 (5)
F13	7463 (22)	4840 (12)	137 (6)	C13	4883 (17)	7841 (9)	1498 (5)
F14	5748 (23)	2931 (12)	41 (6)	C14	3658 (13)	8057 (9)	1498 (5)
F15	5443 (16)	4446 (13)	262 (6)	C15	2799 (14)	8654 (8)	1417 (5)
F16	7738 (22)	3226 (16)	−77 (6)	C16	3307 (15)	9444 (13)	1093 (6)
F21	997 (14)	1038 (19)	2674 (5)	C17	883 (16)	7711 (11)	1654 (6)
F22	1414 (10)	953 (11)	1926 (5)	C18	546 (15)	9153 (11)	1153 (5)
F23	18 (16)	−93 (8)	2237 (5)	C19	−1 (18)	8634 (11)	744 (5)
F24	−1105 (11)	1103 (9)	2545 (4)	C20	946 (18)	8160 (15)	440 (7)
F25	−683 (10)	1088 (12)	1796 (4)	C21	278 (20)	7609 (15)	37 (6)
F26	286 (14)	2192 (8)	2250 (5)	C22	1273 (19)	6828 (16)	−165 (6)
N1	4046 (10)	7079 (8)	2337 (4)	C23	1757 (21)	6044 (16)	118 (6)
N2	4177 (10)	5100 (8)	2316 (4)	C24	618 (25)	5420 (26)	308 (13)
N3	5793 (10)	5157 (9)	1619 (4)	C25A	1489 (32)	5099 (24)	810 (11)
N4	5623 (10)	7152 (9)	1637 (4)	C25B	1288 (37)	4457 (27)	543 (13)
N5	1489 (12)	8523 (8)	1421 (4)	C26A	437 (27)	4660 (20)	1149 (10)
N6	1745 (15)	3566 (11)	1412 (5)	C26B	228 (33)	3904 (26)	753 (11)
C1	2639 (14)	8476 (9)	2447 (5)	C27	1021 (18)	4294 (13)	1643 (7)
C2	3421 (13)	7784 (9)	2152 (5)	C28	968 (28)	2862 (19)	1113 (10)
C3	4058 (14)	6994 (10)	2830 (4)	C29	3124 (17)	3500 (13)	1388 (6)
C4	4808 (13)	6106 (12)	2992 (5)	C30	3722 (20)	2810 (13)	1059 (6)
C5	4209 (16)	5179 (11)	2811 (5)	C1A	7959 (33)	1331 (16)	744 (9)
C6	3646 (13)	4354 (9)	2129 (5)	C2A	7325 (21)	500 (15)	934 (7)
C7	2913 (18)	3613 (11)	2403 (6)	N1A	6929 (18)	−164 (15)	1095 (7)

Calcd for $C_{29}H_{50}N_6NiP_2F_{12}$: C, 41.80; H, 6.06; N, 10.11. Found: C, 42.27; H, 6.21; N, 10.46. A final recrystallization from acetonitrile/ethanol gave orange needles that were found to be twinned. Replacement of acetonitrile by acetone in the recrystallization solvent mixture produced diffraction-quality crystals in the form of orange-brown blocks.

[(2,3,14,15,17,23-Hexamethyl-3,14,18,22,25,29-hexaazabicyclo-[14.7.7]triaconta-1,15,17,22,24,29-hexaene-κ^4N)nickel(II)] Hexafluorophosphate (10). This complex was prepared by using the procedure described for the preceding reaction, with 1.7 g of 1,10-bis(*p*-tolylsulfonyl)decane (3.3 mmol) dissolved in 250 mL of a 3:1 acetonitrile/tetrahydrofuran mixture, 2.3 g of [Ni(MeNEthi)$_2$[16]cyclidene](PF$_6$)$_2$ dissolved in 240 mL of acetonitrile, and 0.17 g of sodium metal. Total dripping time was 6 h, and total reaction time was 36 h. The product was purified twice by column chromatography, and crystallized from an acetonitrile/methanol solution. Yield: 1.0 g (36%). Anal. Calcd for $C_{30}H_{52}N_6NiP_2F_{12}\cdot CH_3CN$: C, 42.58; H, 6.34; N, 11.21. Found: C, 42.77; H, 6.45; N, 11.34. Slow evaporation of an acetonitrile/ethanol solution of the complex resulted in the formation of orange-brown blocks suitable for structure analysis.

Other complexes were prepared according to previously published procedures.[1,11]

NMR Measurements. ^{13}C NMR data was collected by using Bruker AM500 or Varian XT-300 spectrometers operating at 125.76 and 75.48 MHz, respectively. Deuterated acetonitrile was used as the solvent for all experiments, and the peak at 1.3 ppm was employed as an internal reference vs TMS. Measurements were made at 300 K unless otherwise noted. Assignment of specific resonances was accomplished by using 2-D NMR techniques[16] to correlate ^{13}C resonances with corresponding ^1H signals in the previously assigned proton NMR spectra.[5] For some complexes, unambiguous assignment of the bridging methylene carbons

(16) Meade, T. J. Ph.D. Thesis, The Ohio State University, 1984.

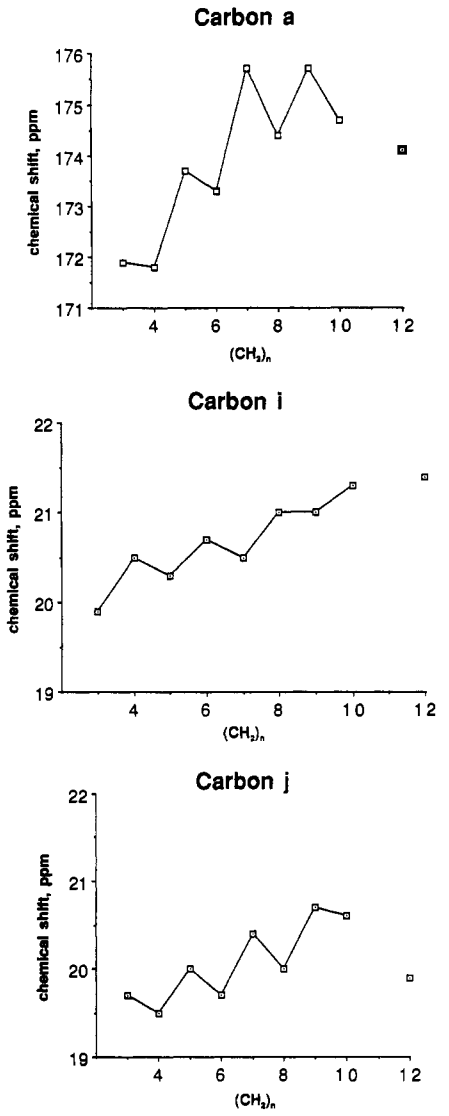

Figure 12. Variation of ^{13}C chemical shift with n for carbon atoms a, i, and j.

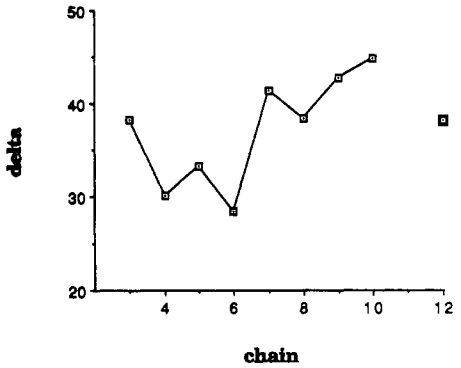

Figure 13. Variation of torsion angle δ (C2–C3–C4–N3) with chain length. Values for **9** and **10** are from present work, and others are from ref 1; values are averaged over all complexes not containing coordinated axial ligands.

was not possible with this technique due to lack of resolution in the proton spectra for these resonances. A full list of ^{13}C NMR chemical shift values for the polymethylene-bridged Ni(II) complexes where n = 3–10 and 12 is presented in Table III. Low-temperature data for selected resonances for **9**, **10**, and **12** are in Table IV.

Crystallographic Analysis. The crystal structures of complexes **8** and **12** have been reported previously.[1] Crystal data for complexes **9** and **10** are listed in Table V. Data collection and refinement were as follows (data for **10** in brackets): Data were collected with a Nicolet $P2_1$ four-circle diffractometer in the ω–2θ mode using graphite-monochromatized Mo Kα radiation. Maximum 2θ was 48° [50°] with scan range (2θ) ± 1.1° [1.0] around the Kα_1–Kα_2 angles and scan speed 3 [4]–29° min^{-1}, depending on the intensity of a 2-s prescan; backgrounds were measured at each end of the scan for 0.25 of the scan time. *hkl* ranges were 0/12, −14/14, and −15/15 [0/12, 0/16, and 0/32]. Three standard reflections were monitored every 200 reflections and showed 4% [5%] decay during data collection: The data were corrected for this. Unit cell dimensions and standard deviations were obtained by least-squares fit to 15 reflections ($15 < 2\theta < 18°$ [$20 < 2\theta < 22°$]). Reflections were processed by using profile analysis to give 6388 [4051] unique reflections; 3526 [2526] were considered observed ($I/\sigma(I) \geq 2.0$) and used in refinement; they were corrected for Lorentz, polarization, and absorption effects, the last by the Gaussian method. Maximum and minimum transmission factors were 0.93 and 0.87 [not provided by the program for **10**].

Anisotropic temperature factors were used for all non-hydrogen atoms, except solvent and disordered atoms. Hydrogen atoms were given fixed isotropic temperature factors, U = 0.07 Å^2. Those defined by the molecular geometry were inserted at calculated positions and not refined (omitting those attached to disordered atoms); methyl groups were treated as rigid CH_3 units. Final refinement was on F by least-squares methods, refining 475 (476) parameters. Largest positive and negative peaks on a final Fourier synthesis were of height 0.8 and −0.6 (±0.8) e Å^{-3}. A weightng scheme of the form $W = 1/(\sigma^2(F) + \gamma F^2)$ with γ = 0.0021 [0.0019] was used and shown to be satisfactory by a weight analysis. Maximum shift errors in the final cycle were 1.1 for the thermal parameter of a disordered C atom for **9** and 0.5 for that of **10**. Computing was with SHEXTL PLUS[17] on a DEC Microvax-II. Scattering factors in the analytical form and anomalous dispersion factors were taken from ref 18. Final atomic coordinates are given in Table VI.

For **9**, no systematic absences were observed and the space group $P\bar{1}$ was assumed. The structure was solved by direct methods (TREF in SHEXTL PLUS); one molecule of solvent acetone was located. Three chain atoms were found to be disordered, and after an investigation of various models using linked occupancies, all the disordered atoms were given 0.5 fixed occupancies.

For **10**, systematic absences *h*00, $h \neq 2n$; 0*k*0, $k \neq 2n$; and 00*l*, $l \neq 2n$ indicate space group $P2_12_12_1$. Heavy atoms were located by the Patterson interpretation section of SHEXTL, and the light atoms were then found on successive Fourier syntheses. The chain atoms C25 and C26 are disordered and were given linked occupancies, refined to 0.54(a):0.46(b). The large thermal parameters for C24 suggest that it is also somewhat disordered, although not to the extent of having resolved positions. A *df″* multiplier refinement gave a value of 0.09 (0.14), indicating that the crystals show "inversion twinning", with a mixture of domains of both chiralities.

Acknowledgment. The financial support of the U.S. National Institutes of Health, Grant No. GM10040, and of the U.S. National Science Foundation, Grant No. 8822822, is greatly appreciated. The Ohio State University (The University of Kansas) and University of Warwick collaboration has been supported by a NATO travel grant.

Supplementary Material Available: Listings of full bond lengths and angles, anisotropic thermal parameters, and H atom coordinates for **9** and **10** (8 pages); listings of structure factors for **9** and **10** (38 pages). Ordering information is given on any current masthead page.

(17) Sheldrick, G. M. *SHEXTL PLUS: User's Manual*; Nicolet Instrument Co.: Madison, WI, 1986.

(18) *International Tables for X-ray Crystallography*; Kynoch: Birmingham, England, 1974; Vol. IV.